ACS APPLIED MATERIALS & INTERFACES

www.acsami.org

Research Article

Integration of Gold Nanoparticle–Carbon Nanotube Composite for Enhanced Contact Lifetime of Microelectromechanical Switches with Very Low Contact Resistance

Eunhwan Jo,[‖] Yong-Bok Lee,[‖] Yohan Jung, Su-Bon Kim, Yunsung Kang, Min-Ho Seo, Jun-Bo Yoon,* and Jongbaeg Kim*

Cite This: *ACS Appl. Mater. Interfaces* 2021, 13, 16959–16967

Read Online

ACCESS | Metrics & More | Article Recommendations | Supporting Information

ABSTRACT: Electrical circuits require ideal switches with low power consumption for future electronic applications. However, transistors, the most developed electrical switches available currently, have certain fundamental limitations such as increased leakage current and limited subthreshold swing. To overcome these limitations, micromechanical switches have been extensively studied; however, it is challenging to develop micromechanical switches with high endurance and low contact resistance. This study demonstrates highly reliable micro-electromechanical switches using nanocomposites. Nanocomposites consisting of gold nanoparticles (Au NPs) and carbon nanotubes (CNTs) are coated on contact electrodes as contact surfaces through a scalable and solution-based fabrication process. While deformable CNTs in the nanocomposite increase the effective contact area under mechanical loads, highly conductive Au NPs provide current paths with low contact resistance between CNTs. Given these advantages, the switches exhibit robust switching operations over 5 × 10^6 cycles under hot-switching conditions in air. The switches also show low contact resistance without subthreshold region, an extremely small leakage current, and a high on/off ratio.

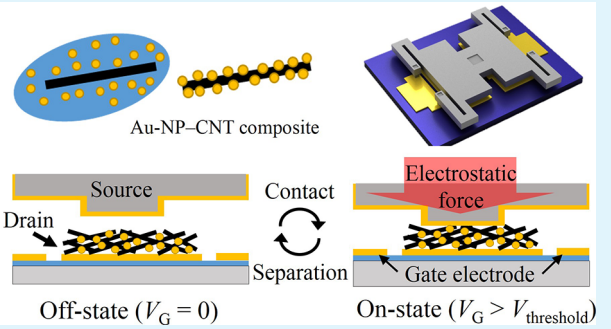

KEYWORDS: *carbon nanotube, gold nanoparticle, microelectromechanical system, mechanical switch, reliability*

1. INTRODUCTION

Electrical circuits have consistently needed ideal and reliable switches with low power consumption for advanced electronic applications such as zero-standby-power integrated circuits for the internet of things, radiofrequency (RF) signal transmission devices for telecommunication systems, and environment-independent logic applications in the automobile and aerospace industries.[1−3] However, transistors, which have driven the industrial development of more functional and mass-producible electronic devices, have suffered from fundamental limitations, such as a theoretically minimum subthreshold swing value of 60 mV/dec at room temperature,[4] increased leakage power consumption resulting from scaling,[5] and performance degradation owing to external environments.[6] Micro-electro-mechanical (MEM) switches have attracted interest as a promising means to overcome these limitations of transistors.[1] MEM switches connect and break an electrical circuit, respectively, through contact and separation between the contact surfaces of two terminals. There is no subthreshold conduction path in MEM switches owing to the physical gap in the off state. Accordingly, MEM switches theoretically have ideal switching performances such as an infinite subthreshold slope, zero leakage current, and an extremely high on/off ratio.

However, practical applications of MEM switches have been limited because of their low contact reliability. Owing to its low contact resistance and high conductivity, gold (Au) has been used as a contact material, either in bulk or as thin films, for MEM switches. Despite their superior electrical properties, MEM switches based on Au have a limited contact lifetime because of the poor mechanical properties of Au (such as a low Young's modulus, low hardness, and low melting temperature).[7] In particular, in the hot-switching condition, repeated contact causes damage to the Au surface, including wear, material transfer, melting, and welding.[7,8] Hard conductive materials exhibiting excellent mechanical properties are among the various solid contact materials that have been used to replace Au and develop reliable MEM switches.[3,9−14] For example, He et al. reported nano-electro-mechanical (NEM) switches and logic gates based on silicon carbide and achieved

Received: December 13, 2020
Accepted: March 23, 2021
Published: April 2, 2021

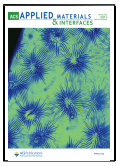

Table 1. Comparison of Reported Nano-/Micro-Electro-Mechanical (NEM/MEM) Switches to Improve a Contact Reliability

materials (contact)	cycles	ambient condition	on-state current	on-state resistance (Ω)	switching-on voltage (V)	fabrication temperature	actuation direction	ref
silicon carbide (SiC) (SiC-to-SiC)	2.0×10^{10}	air	10 nA	10^4	6	900 °C	in-plane	3,15,16
titanium oxide (TiO_2) (TiO_2-to-TiO_2)	1.25×10^9	N_2	0.1 mA	10^4	5.35	CMOS-compatible	out-of-plane	17
graphene (GR) (GR-to-GR)	3×10^6	vacuum	1 μA	4×10^3	85	900 °C	in-plane	19
nanocrystalline graphite (NCG) (NCG-to-NCG)	2.8×10^6	air	3 μA	1.7×10^4	18.7	750 °C	in-plane	20
vertically aligned CNT (VACNT) (VACNT-to-VACNT)	1×10^6	air	10 mA	285	52	700 °C	in-plane	21
noble-metal NPs (metal NPs-to-Au)	1×10^5	air	1 μA	1				22−24
Au NPs (Au NPs-to-Au)	4.75×10^5	air	N/A	2.5	56.3	CMOS-compatible	out-of-plane	25
Au−CNT composite (Au-to-Au)	9×10^3					CMOS-compatible	out-of-plane	26
CNT network (CNT-to-Au)	7×10^8	N_2	0.1 mA	12.7	71.8	CMOS-compatible	out-of-plane	27
this work (Au-NP-decorated CNT-to-Au)	5×10^6	air	1 μA	12.19	25.2	CMOS-compatible	out-of-plane	this work

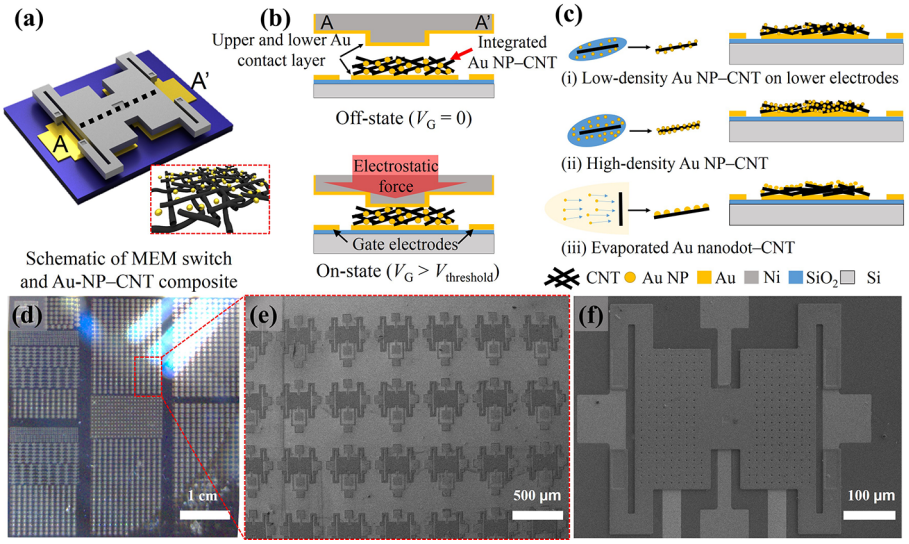

Figure 1. (a) Schematic of three-terminal microelectromechanical (MEM) switch based on Au-NP−CNT composite. (b) Cross-sectional view (A−A′) of the switch with the composite at off and on states. (c) Schematic diagrams of nanocomposites with isotropically coated (i) low-density and (ii) high-density Au NPs on the patterned CNT network, and (iii) Au nanodots deposited on the top surface of the CNT network by evaporation. (d) Optical image of the switch array indicating mass reproducibility of the proposed manufacturing process. (e) Enlarged SEM image of the switch array. (f) SEM image of a single switch.

high contact reliability under hot-switching conditions in ambient air[15,16] Kam et al. also reported a durable NEM switch by adopting a tungsten electrode coated with titanium oxide, showing over 1 billion cycles under hot-switching conditions in a nitrogen environment.[17] However, they exhibit a high contact resistance, on the order of several kilo-ohms, regardless of their conductivity. This is because switches based on hard materials have a small effective contact area owing to their lack of deformability under contact forces.[18] Moreover, some metals and compounds may not be suitable as contact materials for switches for RF applications because using switches with a contact resistance greater than 5 Ω could result in insertion loss.[1]

Recently, nanomaterials such as zero-dimensional (0D) nanoparticles (NPs), one-dimensional (1D) nanotubes, and two-dimensional (2D) nanosheets with unique characteristics have been explored as contact materials to improve contact reliability and reduce the electrical contact resistance of mechanical switches as listed in Table 1.[19−27] However, adopting carbon nanomaterials, including 1D carbon nanotubes (CNT), 2D graphene, and nanocrystalline graphite on MEM switches, leads to increased contact resistance owing to the low electrical conductivity of the sp^2-bonded carbon network in the out-of-plane direction.[28,29] Meanwhile, noble metal NPs have attracted attention as contact materials to enhance the switching performance of MEM switches through a decrease in contact resistance and an improvement in repeatability.[22−25] Among these metal NPs, a switch adopting Au NPs has been implemented. However, its contact lifetime was still limited to less than 5×10^5 cycles owing to the poor mechanical properties of Au NPs, which is insufficient even for applications requiring a relatively short contact lifetime, such as communication systems.[1] In this study, we demonstrate MEM switches with Au-NP−CNT composites fabricated through a simple, scalable, and low-temperature process. The adoption of a CNT network with Au NPs for the contact surface combines

https://doi.org/10.1021/acsami.0c22084
ACS Appl. Mater. Interfaces 2021, 13, 16959−16967

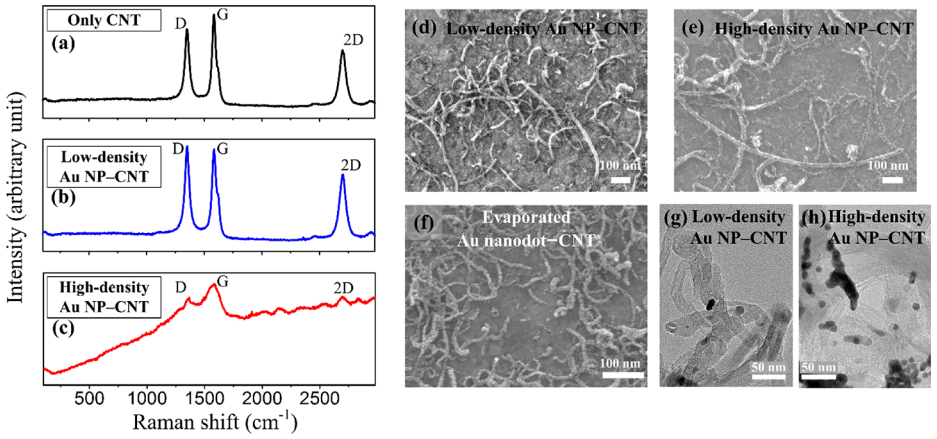

Figure 2. (a) Raman spectra of a CNT network and (b) low- and (c) high-density Au-NP−CNT composites. Raman spectra of the CNT and composites exhibit disorder-induced D band, tangential G band, and 2D band, respectively. The gradual increase in the Raman shift in (c) indicates that photon excitation occurred and acted as a screening mirror effect in high-density Au NPs. (d, e) SEM images, respectively, of low- and high-density Au-NP−CNT composites showing isotropic deposition of Au NPs on individual CNTs. (f) SEM image of directionally deposited Au nanodots on the CNT network by e-beam evaporation. (g, h) Tunneling electron microscopy (TEM) images, respectively, of low- and high-density Au-NP−CNT composites.

the advantages of two nanomaterials, namely, the deformability of CNTs at contact forces and the low contact resistivity of Au NPs. Therefore, the reliability and device performance of the MEM switch were improved. The switch with nanocomposites exhibited highly improved reliability over 5×10^6 cycles under the hot-switching condition and ideal switching performances such as low contact resistance, an abrupt subthreshold slope, extremely small leakage current, and a high on/off ratio. The change in the switching characteristics related to the density and orientation of Au NPs deposited on CNTs was also investigated.

2. RESULT AND DISCUSSION

2.1. Switch Fabrication and Operation Concept.

Figure 1a shows the conceptual schematics of the proposed MEM switch based on the Au-NP−CNT composite. The switch operates as a three-terminal device and consists of an upper movable drain plate with four crab legs, a lower static gate electrode, and a lower fixed source electrode with the Au-NP−CNT composite contact area. The upper plate, suspended on the four crab legs, is bent downward by electrostatic force induced by the potential difference between the fixed gate and movable drain electrode. Then, the switch establishes a contact when a gate voltage (V_G) is applied over the threshold voltage, as shown in Figure 1b. The fabrication process of the MEM switch is similar to that reported in the previous work,[27,30] except for the process for depositing Au NPs. The details of the fabrication process are described in the Experimental Section and Figure S1. Figure 1c shows a schematic of the deposition of Au NPs on the prepatterned CNT network. To investigate the effect of Au NP deposition on switching characteristics such as the resistance, contact behavior, and contact lifetimes of switches, the density of Au NPs in nanocomposites was adjusted by the amount of the Au colloidal solution having the same concentration, as shown in Figure 1c-i,ii. For the high-density Au NPs−CNT composite, the Au NP solution was dried slowly at a low temperature of 40 °C for 2 h to prevent a "coffee-ring effect" of Au NPs.[31] The Au-NP-coated wafers were then baked at 110 °C to remove the residual solvent and enhance the interfacial adhesion of the composite. Through the coating and drying processes, Au NPs were coated on all sides of the individual CNTs. We chose a dispersed solution of 10 nm diameter Au NPs, smaller than the thickness of CNTs (20 nm), to utilize both CNTs and Au NPs as the contact material when the switch forms contact. Furthermore, we fabricated the switch with the Au nanodots−CNT composite to compare the switching characteristics with the direction of deposited Au NPs. The individually isolated Au was coated as a type of nanodot on the top surface of the CNT network by e-beam evaporation, as shown in Figure 1c-iii. Figure 1d shows an optical image of the fabricated switch array. The batch-fabricated switch array indicates that the proposed fabrication process can be used for mass production. Figure 1e,f shows enlarged scanning electron microscopy (SEM) images of the array and single device, respectively. Figure S2 and Table S1 list all the device parameters and measured dimensions.

Figure 2a−c shows the Raman spectra of the CNT network without Au NPs and low- and high-density Au-NP−CNT composites after the entire fabrication process. The Raman spectra of the CNTs exhibit disorder-induced D and tangential G band with an intensity ratio (I_D/I_G) of approximately 0.85 (Figure 2b). Figure 2b shows the Raman spectra of the low-density Au-NP−CNT composite with a slightly increased I_D/I_G ratio of approximately 1.03, indicating a modification of the CNT surface and enhancement of plasmonic scattering by Au NP decoration.[32] However, the intensity in Raman spectra of the high-density Au NP−CNT composite gradually increases as the wavenumber (cm^{-1}) increases with the weak D and G bands, as shown in Figure 2c. This tendency implies that the high-density Au NPs acted as a screening mirror and photon excitation occurred, which is similar to the previously reported result.[33] Figure 2d,e shows the SEM images of the low- and high-density Au-NP−CNT composites. The Au NPs infiltrated into the CNT network and were isotropically decorated on the individual CNTs with different densities by the solution-based coating method. Compared with the solution-based Au NP decoration on CNTs, Au nanodots were deposited only on the top surfaces of the CNT network owing to the directionality of the e-beam evaporation, as shown in Figure 2f. Figure S3a−c shows the SEM images of Au deposited on CNTs with thicknesses of 2, 5, and 10 nm. Au has the shape of nanodots

https://doi.org/10.1021/acsami.0c22084
ACS Appl. Mater. Interfaces 2021, 13, 16959−16967

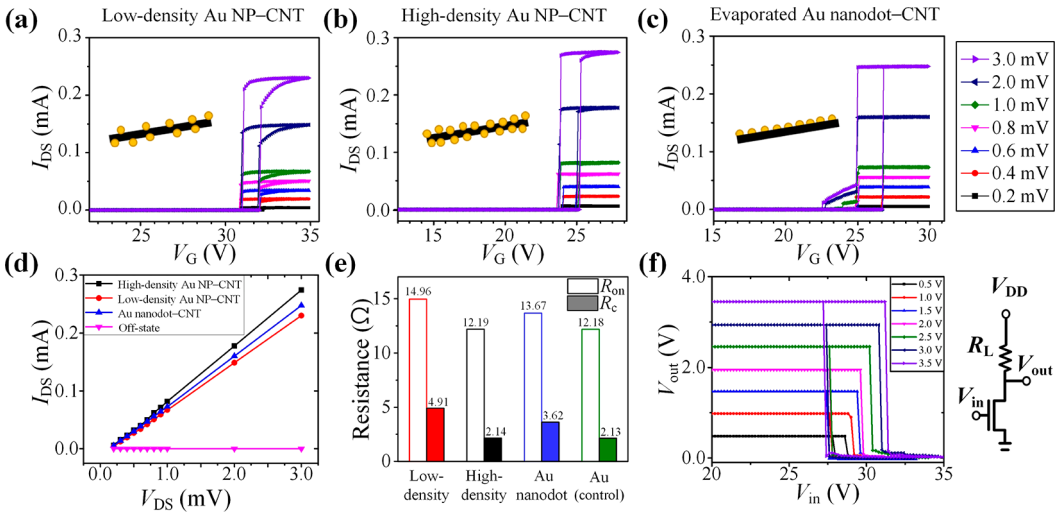

Figure 3. Electrical characteristics of MEM switches. Measured drain–source current (I_{DS}) versus applied gate voltage (V_G) curves of the switch with (a) low- and (b) high-density Au-NP–CNT and (c) Au-nanodot–CNT composites. Bias drain–source voltages (V_{DS}) from 0.2 to 3.0 mV were applied during the V_G sweep. (d) I_{DS}–V_{DS} curves indicating the contact between the composite and the upper Au layer is ohmic. (e) On-state resistance and extracted contact resistance of fabricated switches. (f) Voltage transfer characteristic of MEM inverter using high-density Au-NP–CNT switch showing repeatable and abrupt voltage changes.

up to the thickness of 5 nm; at greater thicknesses, it forms a polycrystalline thin film, as shown in Figure S3c,d and reported in previous work.[34] Figure 2g,h show the transmission electron microscopy (TEM) images of the low- and high-density 10 nm diameter Au NPs on the CNT network. It is seen that the Au NPs infiltrated into the CNT network with different densities.

2.2. Characterization of Switches. The hysteretic switching characteristics of the switches were measured to investigate the contact behaviors of the Au-NP-decorated CNTs. Figure 3a,b shows the measured drain–source current (I_{DS}) versus V_G sweep curves of the low- and high-density Au-NP–CNT composites with bias drain–source voltages (V_{DS}) from 0.2 to 3.0 mV in air. All the switches were operated without pull-in instability because the designed movable distance of the upper electrode (g_d) was shorter than one-third of the gap between the plate and lower gate electrode (g_0), as illustrated in Figure S1.[27,35] Therefore, the contact force increased monotonically with an increase in the applied gate voltage. Typical MEM switches using a solid conductive contact material exhibit a steep current increase from near zero, which then remains constant although V_G increases further, as shown in Figure S4a. However, the switch with CNTs exhibited a gradual increase in I_{DS} with high contact resistance after contact owing to the deformability of CNTs under the applied contact force, as shown in Figure S4b. In contrast, the switch with the Au-NP-decorated CNTs showed an increase in both I_{DS} and deformable contact behavior under increased contact force. As shown in Figure 3a, the switch with the low-density Au-NP–CNT composite showed a sharp increase in I_{DS} at the turn-on gate voltage (V_{on}) of 32.0 V with the on-state resistance (R_{on}) of 20.2 Ω and an on/off ratio larger than 10^7 at 10 mV bias voltage. R_{on} further decreased to 14.96 Ω as V_G increased, showing the increase in the effective contact area in a designated contact area (16 μm × 16 μm) owing to the deformability of CNTs.[18] Figure 3b shows the measured I_{DS} versus V_G sweep curves of the switch with the high-density Au-NP–CNT composite. In the I_{DS}–V_G sweep curves, R_{on} slightly decreased from 12.6 to 12.2 Ω as V_G increased from 25.2 V. This result indicates that the increase in Au NPs provided a sufficient current path at the contact interface; thus, R_{on} slightly decreased even though the deformable CNTs increased the effective contact area.

However, the I_{DS} of the switch with the Au-nanodot–CNT composite sharply increased at V_G of 26.8 V and did not change even for the increased contact force by applying additional V_G, as shown in Figure 3c. This result indicates that the thin Au nanodots on the CNTs formed Au-to-Au contact with the upper contact electrode without the involvement of CNTs. Thus, the hysteretic switching behavior of the switch with the Au-nanodot–CNT composite is similar to that of the typical Au-based switches. However, the switch with the Au-nanodot–CNT composite showed unstable adhesion force at the contact interface even during 10 cycles of repeated operations. When I_{DS}–V_G sweep curves were measured at 0.2–0.8 mV bias V_{DS}, there was no significant change in V_{on} or turn-off gate voltage (V_{off}). However, the switch with the Au-nanodot–CNT composite exhibited an unstable V_{off} in the reverse sweep of V_G after 8 operation cycles. V_{off} represents the adhesion force between the contact interfaces at constant V_{on} because the switch operated without the pull-in phenomenon.[27,35] In the reverse sweep of V_G, I_{DS} reduced from approximately 72.5 μA to approximately 13.7 μA, and the upper contact electrode was not detached completely from the lower electrode. This is because the elastic restoring force of the beams is lower than the sum of the electrostatic and adhesion forces. The unstable V_{off} and I_{DS} were attributed to the increased adhesion force. The thin Au nanodot melted by Joule heat under the hot-switching condition and caused welding; thereby, the switch with the Au-nanodot–CNT composite was not completely detached owing to the increased adhesion force at the weld interface. In contrast, the switches with low- and high-density Au NPs–CNT composites both showed reliable contact and separation behaviors after repeated cycles and varying bias V_{DS} because of current density distribution resulting from the infiltrated Au NPs on the deformable CNT network.

To investigate the contact properties with respect to the Au NP solution's concentration per unit area, we prepared four

https://doi.org/10.1021/acsami.0c22084
ACS Appl. Mater. Interfaces 2021, 13, 16959–16967

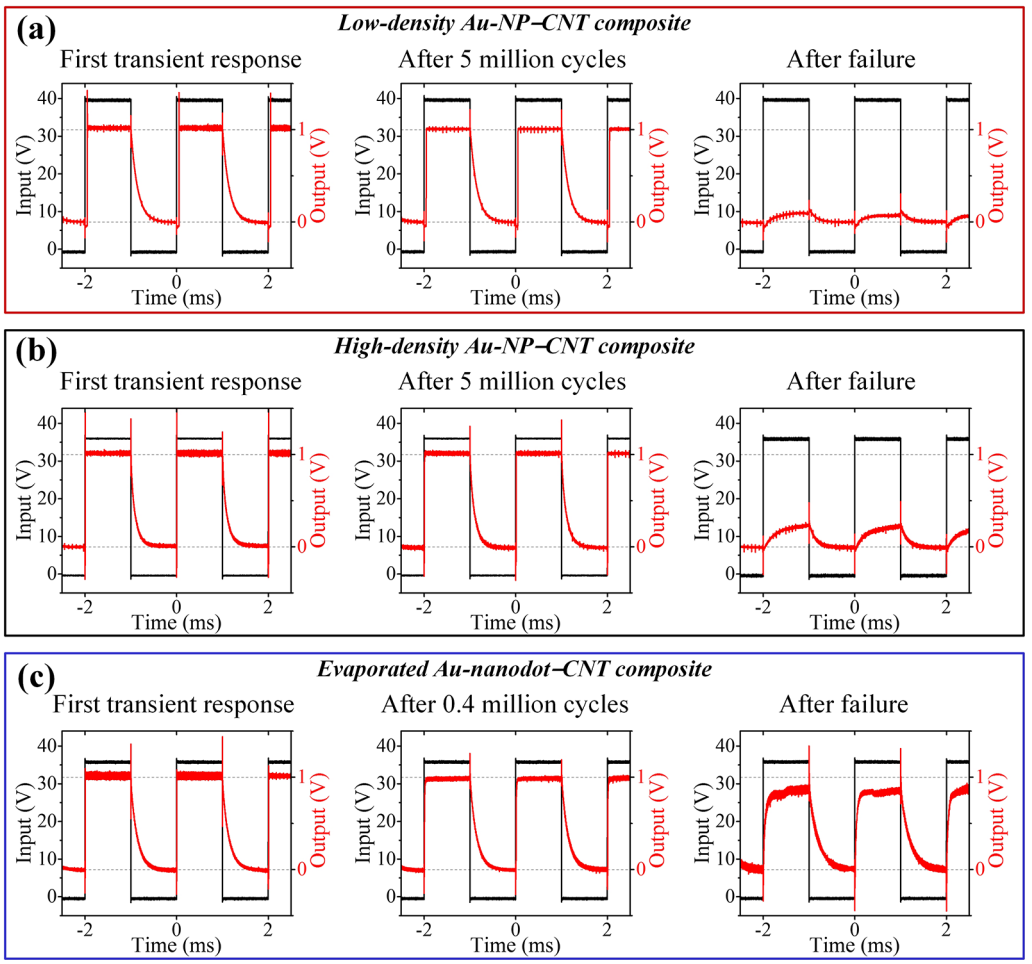

Figure 4. Lifetime measurement of MEM switches with nanocomposites under hot-switching conditions. Transient responses of the switch with (a) low- and (b) high-density Au-NP−CNT composites and (c) Au-nanodot−CNT composite at the first operation, as well as right before and immediately after the failure. Responses were observed under hot-switching conditions by an oscilloscope with an applied bias V_{DS} of 1 V and an external resistor of 1 MΩ.

different specimens with identical concentrations of CNTs and four different concentrations of Au NP coating (0.2, 10, 100, and 400 mg/cm^2, respectively). To perform an experiment similar to the contact conditions of the switch, we used an Au-coated microrod with a 20 μm diameter hemisphere to approximate the contact area of the switch (16 μm × 16 μm). Then, we measured the electrical resistances at the Au electrodes (100 μm × 100 μm) by applying a contact force of 1 mN, which is comparable to the magnitude of the electrostatic force when the V_G is 65 V. The z-axis displacement and contact force were controlled by an electrical push−pull tester (KMX-E100N, MAS) and a force gauge (DTG-10, Digitech), respectively. We measured the electrical resistance through a source meter (2614B, Keithley) while applying the bias voltage of 0.5 mV. Figure S5a,b shows the schematic of the microcontact apparatus and the averaged electrical contact resistance with respect to the concentration of Au colloidal solutions per unit area in the composites, exhibiting a decrease of contact resistance as the Au NP concentration increases. Each resistance value and its error bar were obtained by measuring five times.

Increasing the Au NP density does not always result in improvement in the switching performance. We examined the change in contact behavior by increasing the Au NP density further. Figure S6a,b show, respectively, the I_{DS}−V_G sweep curves and an SEM image of the switch with the agglomerated Au-NP−CNT composite via double coatings of Au NP solution. For a double coating of Au NPs, we first deposited an approximately 403 mg/cm^2 concentration of Au colloidal solution per unit area and dried the solvent completely. Then, the same amount of Au colloidal solution was deposited and dried again. As a result, the total concentration of the doubly coated Au NP solution per unit area is close to 800 mg/cm^2. Through these two Au NP depositions, the agglomerated Au-NP−CNT composite was prepared. The contact occurred at V_G of 15 V, which is smaller than V_G of other switches with a single coating of Au NPs owing to the increased thickness of the Au-NP−CNT composite. I_{DS} increased with an increase in V_G, which implied that the agglomerated Au NPs on the CNTs collapsed and were rearranged under the increased contact force. In the reverse sweep of V_G, I_{DS} remained constant until the upper layer was detached. This indicates that the contact force caused plastic deformation of the composite; thus, the resistance and V_{on} were irreversibly changed. This permanent changes in the composite topography make the V_{on} unpredictable.

Figure 3d shows the I_{DS}−V_{DS} curves of the switches after the contact area was saturated under contact forces. The linear I_{DS}−V_{DS} curves indicate that the lower composite-to-upper Au layer contact is ohmic even at the submillivolt scale. Figure 3e

https://doi.org/10.1021/acsami.0c22084
ACS Appl. Mater. Interfaces 2021, 13, 16959−16967

shows R_{on} and extracted contact resistance (R_c) of the switches. The R_{on} and R_c of the switches with low- and high-density Au-NP−CNTs and Au-nanodot−CNT composite are 14.96, 12.19, and 13.67 Ω and 4.91, 2.14, and 3.62 Ω, respectively. The R_{on} and R_c of the switch without the nanocomposite (Au-to-Au contact) are 12.18 and 2.13 Ω, respectively, as shown in Figure S4a. These results imply that the contact resistance of the high-density Au-NP−CNT composite can fall in the range of the contact resistance of the Au thin film. Figure S7 shows the calculation of R_c to remove the resistance resulting from the electrodes and measurement equipment. The low contact resistance of the switch with the composite also indicates that the proposed switch could be used for RF applications that require contact resistances below 5 Ω.[1] Figure 3f shows the voltage transfer characteristics of a unipolar MEM inverter corresponding to supply voltages (V_{DD}) from 0.5 to 3.5 V and a circuit schematic of the unipolar MEM inverter for an application. The MEM inverter showed outstanding performance with an extremely low off state and subthreshold swing with abrupt transitions while exhibiting repeatable operations owing to the stable adhesion force at contact interfaces.

The fabricated switches have a high operating voltage owing to the wide gap and the large stiffness of the spring. Recently, many studies have been conducted to develop low-voltage operating switches. Among them, we anticipate that the following three representative strategies achieving the low operational voltage of 1 V or less could be introduced into our switches operating in an out-of-plane direction: (i) reducing the gap of the switch significantly;[36] (ii) introducing other driving methods that could apply a force higher than electrostatic force, such as a phase transition,[37] thermal,[38] or piezoelectric operation;[39] and (iii) adjusting the actuation voltage by operating it as a 4-terminal device with a body electrode.[40,41]

Moreover, the size of the switch with a length of about 430 μm is significantly large compared with that of the transistor, which aims to reach a footprint of less than 40 nm.[42] To the best of our knowledge, the smallest mechanical switch with the device length of 300 nm has been reported,[43] but it still has a larger size compared to those of transistors. In other words, it is expected to be challenging to have a size smaller than that of a transistor. However, our mechanical switches show near-zero standby power consumption[44] and the low contact resistance of less than 5 ohms required for RF switches. Therefore, we expect that it could be integrated into transistor-based circuits to reduce the standby power of the circuits or used as a switch to transmit RF signals used in the communication field.

In terms of the size reduction of the composite, the patterning size of CNTs and Au NPs is determined by the resolution of the lithography and lift-off processes, respectively. For example, Lee et al. reported a 3D fin-structured CNT-FET. They fabricated a CNT-coated fin structure with a width of 100 nm through a solution-based CNT deposition process.[45] Wang et al. also demonstrated a 50 nm wide line pattern made of Au NPs by using the gold colloidal solution coating and lift-off processes.[46] The methods of integrating CNT and Au NPs reported in the above literature are similar to those of this work. Therefore, it is expected that the area size of the Au-NP−CNT composite can be reduced to a submicrometer scale by optimizing the fabrication process.

2.3. Measurements of Contact Lifetime. We measured the contact lifetimes of the MEM switches with nanocomposites under the hot-switching condition. A 1 V bias V_{DS} was applied with a 1 MΩ external resistor to control I_{DS} of the switches. We also monitored the transient response of the switches through an oscilloscope. Figure S8 presents the experimental setup of an electrical circuit and equipment measuring the lifetime. Figure 4a shows the transient response of the switch with the low-density Au-NP−CNT composite at first cycles and immediately before and after failure by applying a 500 Hz square wave V_G of 40 V with a 50% duty ratio in air. The transient curves indicate no output degradation and distortion even at the high-frequency operation for 5×10^6 cycles. Figure 4b shows the transient response of the switch with the high-density Au-NP−CNT composite by applying a 500 Hz square wave V_G of 36 V. The output voltage remained constant for 5×10^6 cycles, which is similar to that of the switch with the low-density Au-NP−CNT composite. Figures S9 and S10 show the transient responses of the switches with low- and high-density Au-NP−CNT composites to verify the reliable operations of the switches. We measured the transient responses at every 5×10^5 cycles from the initial contact to 2×10^6 cycles, and then at every 1×10^6 cycles from 2×10^6 cycles to failure. The gradual decrease in the output voltage at turn-off is an electrical delay induced by the 1 MΩ external resistor.[40] We also monitored the hysteretic switching characteristics periodically for 5×10^6 cycles at the delivering current of 1 uA to verify the contact reliability of the switch with Au-NP−CNT. Figure S11 shows the drain-source current (I_{DS}) with respect to the gate voltage (V_G) sweep curves at the V_{DS} of 0.5 mV for 5×10^6 cycles. A V_{DS} of 1 V was applied with a 1 MΩ external resistor. For 5×10^6 hot-switching cycles, there was no significant change in the switching-on voltages and the I_{DS} values. During the reverse sweep, there is a slight difference in the switching-off voltages between operations at the first cycle and after 1×10^6 cycles. This difference in hysteretic switching characteristics may be attributed to the decrease in the adhesion force at the interfaces due to the Joule heating, which affects the capillary force during repeated operations.[47]

After 5×10^6 operation cycles, we observed an unstable and decreased output owing to the damaged contact surface and increased contact resistance. The typical Au-based MEM switch failed before 1×10^6 operation cycles at a few microamperes in air,[7] which is consistent with our previous works.[25,48] However, our switches based on nanocomposites showed remarkably extended lifetimes, several times longer than that of the Au-based switches. When comparing the switch based on Au-NP−CNT composite with the pure-CNT-based switch at the delivering current of 1 uA in air,[48] both types of switches failed due to a rapid increase in the contact resistance resulting from the surface oxidation. On the other hand, the pure-CNT-based switch showed a contact lifetime of 1.5×10^7 cycles with the current density of 1.56 A/cm^2 (8 μm × 8 μm contact area), whereas the switch with Au-NP−CNTs operated for 5×10^6 cycles at the current density of 0.39 A/cm^2 (16 μm × 16 μm contact area) under hot-switching conditions. Although the contact lifetime of the switch with Au-NP−CNT was reduced compared to that of the pure-CNT-based switch, the switch with Au-NP−CNT exhibited a contact resistance of 2.14 ohms, which is 24% lower than that of the pure-CNT-based switch at the V_G smaller than half of the V_G of pure-CNT-based switch. The difference in the contact lifetimes may originate from the lower mechanical strength of Au NPs and the large difference in the applied V_{DS}

https://doi.org/10.1021/acsami.0c22084
ACS Appl. Mater. Interfaces 2021, 13, 16959−16967

(1.0 V in this work and 0.01 V in the previous work). Meanwhile, the switch with the Au-nanodot−CNT composite exhibited a short contact lifetime under the hot-switching condition (Figure 4c). The switch with the Au-nanodot−CNT composite operated stably for 4×10^5 cycles; however, the output signal decreased owing to the increased contact resistance after failure, which is similar to that of typical Au-based switches.

To investigate the contact surface and failure mode of the switch with nanocomposites, we detached the upper movable plate forcibly by breaking the anchor of the switch with a probe tip. Figure 5 shows SEM images of the upper and lower contact surfaces after the failure. We observed material migration in the SEM image of the switch with the low-density Au-NP−CNT composite, as shown in Figure 5a,b. Locally melted Au migrated from the lower surface to the upper surface on the identical contact regions. Figure 5c,d also shows the melted contact surface in the switch with the high-density Au-NP−CNT composite. These results imply that Joule heating occurred during the repeated operation cycles in the hot-switching condition and resulted in the melting of the contact surface. On the basis of these results, it is expected that repeated operations of switches with nanocomposites induced material transfer and melting in contact interfaces, resulting in the damaged surface; thus, the switches failed because of the abruptly increased resistance.

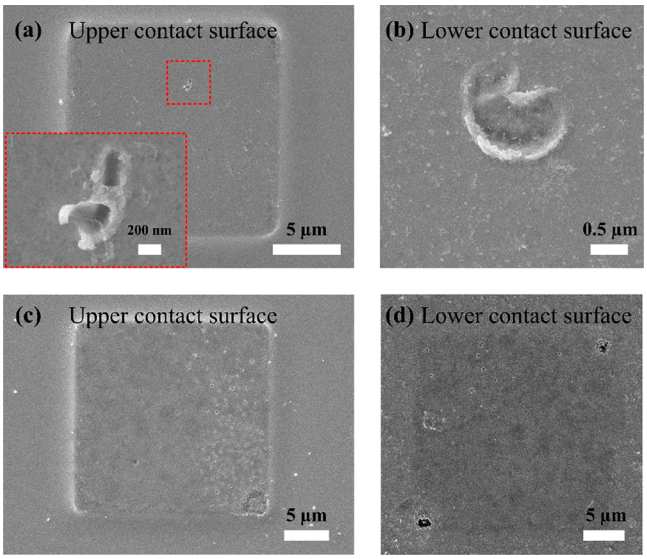

Figure 5. Observation of upper and lower contact areas of the failed MEM switch. (a, b) SEM images of the upper and lower contact areas, respectively, with low-density Au-NP−CNT composites after failure. Material migration from the lower surface to the upper surface on the identical contact region is observed. (c, d) SEM images of the upper and lower contact areas, respectively, with high-density Au-NP−CNT. Melted surface induced by Joule heating during repeated operations is observed.

3. CONCLUSION

We developed reliable MEM switches by integrating Au-NP−CNT nanocomposite on the contact surfaces with a simple, scalable, and solution-based low-temperature process. Deformable CNTs in nanocomposite facilitate an increase in effective contact area under mechanical load, and highly conductive Au NPs provide a current path with low contact resistance between CNTs. By combining these advantages, the fabricated switches showed a robust contact lifetime of approximately 5×10^6 cycles under the hot-switching condition in air. The switches with nanocomposites also exhibited outstanding switching performance such as low contact resistance, extremely low leakage current, high on/off ratio, and steep subthreshold slope. On the basis of the scalable fabrication process and improved reliability, we believe that the Au-NP−CNT nanocomposite can be applied to various contact-based devices to improve their reliability and performance.

4. EXPERIMENTAL SECTION

4.1. Fabrication of Lower Electrodes with a CNT Network. First, 10 nm chromium (Cr) and 100 nm Au were deposited by e-beam evaporation on a thermally oxidized silicon wafer. Cr and Au were then selectively etched using a positive photoresist mask (AZ GXR-601 14 cP, AZ Electronic Materials) and standard metal etchants (Sigma-Aldrich) to form the lower electrodes. The wafer with Au electrodes was dipped in a poly-L-lysine bath (purchased from Sigma-Aldrich) for 5 min after plasma treatment with O_2 flow of 20 sccm and an RF power of 100 W for 90 s (COVANCE-MP, Femto Science) to improve the adhesive capability between Au and CNTs. After rinsing with deionized (DI) water, the wafer was dipped in a prepared 2 mg/mL CNT solution bath for 12 h (previously diluted in *N*,*N*-Dimethylmethanamide solvent with sonication for 6 h). Then, the wafer was rinsed and dried with DI water and a nitrogen gun. The wafer with the CNT-coated Au electrodes was baked at 110 °C on a hot plate for 90 s to completely remove the solvent. The CNTs were patterned by a negative PR mask of 5 μm thickness (DNR-L300, Dongjin Semichem Inc.) and reactive ion etching with O_2 flow of 20 sccm and an RF power of 100 W for 40 s.

4.2. Deposition of Au NPs on a CNT Network. A 10 nm gold colloidal solution suspended in H_2O having the concentration of 5.70×10^{12} molecules/mL was purchased from BBI Solutions. After patterning of a positive PR by an identical photolithography mask used for the CNT patterning, the Au colloidal solution (0.20 and 403.8 mg/cm^2) was coated on the wafer by using spin-coating and drop-casting for low- and high-density Au NPs, respectively. For the high-density Au-NP−CNT composite, the solution was slowly dried at 40 °C in a convection oven to prevent a coffee ring effect. The Au NPs were patterned by using the lift-off method with sonication for 5 min in acetone bath after the wafers were baked at 110 °C on a hot plate for 90 s to remove residual solvent and enhance adhesion between Au NPs and CNT.

4.3. Fabrication of Upper Movable Electrodes. A 400 nm thick gap between the upper contact area and the lower electrodes was formed by patterning the first PR layer. After hard baking, the second PR layer with a thickness of 1.0 μm was then spin-coated and patterned on top of the first layer, forming a 1.4 μm gap between the upper plate and the lower fixed electrodes. After depositing a 100 nm thick Au layer (used as both seed and contact layers) on the entire wafer by e-beam evaporation, an 8 μm thick PR mold (AZ 9260, AZ Electronic Materials) was coated and patterned for nickel (Ni) electroplating. The movable upper electrode was fabricated by electroplating Ni (approximate thickness of 5 μm) as the structural material on the patterned third PR layer. The switches were released with critical point drying after dissolving the three PR layers and Au layers.

4.4. Characterization of MEM Switches. The morphologies and Raman spectra of the Au−CNT composites on the Au electrodes were investigated by using FE-SEM (IT-500HR) and micro-Raman spectrometry (LabRam Aramis, Horiba Jovin Yvon; Ar-ion layer of 532 nm wavelength). The drain−source current versus gate voltage sweep curves with various bias voltages were measured with a source meter (Keithley 2614B, Tektronix). Square wave voltages were applied via a voltage amplifier (F20AD, FLC Electronics) and a function generator (33220A, Agilent). The transient responses of the switches were monitored using an oscilloscope (DSO5014A, Agilent)

https://doi.org/10.1021/acsami.0c22084
ACS Appl. Mater. Interfaces 2021, 13, 16959−16967

at a 1 V bias drain−source voltage applied through a direct current power supply (E3647A, Agilent).

■ ASSOCIATED CONTENT

Supporting Information

The Supporting Information is available free of charge at https://pubs.acs.org/doi/10.1021/acsami.0c22084.

Fabrication process of switches with CNT and Au NPs. SEM image of the switches with geometric parameters. Device parameters and dimensions of the switch. SEM images with difference in deposited thicknesses of Au. Drain−source current (I_{DS}) versus V_G sweep curves of the MEM switch with only Au and CNT. The averaged electrical contact resistance through microcontact apparatus with respect to the concentration of Au colloidal solutions in the composites. I_{DS} versus V_G sweep curve and a SEM image of the switch with agglomerated Au-NP−CNT composite via double coating of Au NP solution. Calculation of contact resistance. Experimental setup for transient responses. Measurement of the transient responses of the switches with low- and high-density Au-NP−CNT composites during repeated operations. I_{DS} with respect to the V_G sweep curves at the V_{DS} of 0.5 mV for cyclic operations of 5×10^6 cycles. (PDF)

■ AUTHOR INFORMATION

Corresponding Authors

Jongbaeg Kim − *School of Mechanical Engineering, Yonsei University, Seoul 03722, Republic of Korea;* orcid.org/0000-0003-4434-5871; Email: kimjb@yonsei.ac.kr

Jun-Bo Yoon − *School of Electrical Engineering, Korea Advanced Institute of Science Technology (KAIST), Daejeon 34141, Republic of Korea;* orcid.org/0000-0002-9447-3807; Email: jbyoon@kaist.ac.kr

Authors

Eunhwan Jo − *School of Mechanical Engineering, Yonsei University, Seoul 03722, Republic of Korea*

Yong-Bok Lee − *School of Electrical Engineering, Korea Advanced Institute of Science Technology (KAIST), Daejeon 34141, Republic of Korea*

Yohan Jung − *School of Mechanical Engineering, Yonsei University, Seoul 03722, Republic of Korea*

Su-Bon Kim − *School of Electrical Engineering, Korea Advanced Institute of Science Technology (KAIST), Daejeon 34141, Republic of Korea*

Yunsung Kang − *School of Mechanical Engineering, Yonsei University, Seoul 03722, Republic of Korea*

Min-Ho Seo − *School of Biomedical Convergence Engineering, College of Information & Biomedical Engineering, Pusan National University, Gyeongsangnam-do 50612, Republic of Korea*

Complete contact information is available at: https://pubs.acs.org/10.1021/acsami.0c22084

Author Contributions

[‖]E.J. and Y.-B.L. contributed equally to this work. The manuscript was written through contributions of all authors. All authors have given approval to the final version of the manuscript.

Notes

The authors declare no competing financial interest.

■ ACKNOWLEDGMENTS

This research was supported by the National Research Foundation of Korea (NRF) funded by Ministry of Science and ICT (MSIT) (grant nos. 2021R1A2B5B03002850 and 2020M3F3A2A01082600).

■ REFERENCES

(1) Rebeiz, G. M.; Muldavin, J. B. RF MEMS Switches and Switch Circuits. *IEEE Microw. Mag.* **2001**, *2*, 59−71.

(2) Qian, Z.; Kang, S.; Rajaram, V.; Cassella, C.; McGruer, N. E.; Rinaldi, M. Zero-Power Infrared Digitizers based on Plasmonically Enhanced Micromechanical Photoswitches. *Nat. Nanotechnol.* **2017**, *12*, 969.

(3) Lee, T.-H.; Bhunia, S.; Mehregany, M. Electromechanical Computing at 500°C with Silicon Carbide. *Science* **2010**, *329*, 1316−1318.

(4) Jiang, C.; Choi, H. W.; Cheng, X.; Ma, H.; Hasko, D.; Nathan, A. Printed Subthreshold Organic Transistors Operating at High Gain and Ultralow Power. *Science* **2019**, *363*, 719−723.

(5) Borkar, S. Design Challenges of Technology Scaling. *IEEE Micro* **1999**, *19*, 23−29.

(6) Neudeck, P.G.; Okojie, R.S.; Chen, L.-Y. High-Temperature Electronics - A Role for Wide Bandgap Semiconductors? *Proc. IEEE* **2002**, *90*, 1065−1076.

(7) Patton, S.; Zabinski, J. Fundamental Studies of Au Contacts in MEMS RF Switches. *Tribol. Lett.* **2005**, *18*, 215−230.

(8) Hyman, D.; Mehregany, M. Contact Physics of Gold Microcontacts for MEMS Switches. *Electr. Contacts* **1998**, 133−140.

(9) Parsa, R.; Lee, W. S.; Shavezipur, M.; Provine, J.; Maboudian, R.; Mitra, S.; Wong, H. P.; Howe, R. T. Laterally Actuated Platinum-Coated Polysilicon NEM Relays. *J. Microelectromech. Syst.* **2013**, *22*, 768−778.

(10) Chen, I. R.; Chen, Y.; Hutin, L.; Pott, V.; Nathanael, R.; Liu, T. J. K. Stable Ruthenium-Contact Relay Technology for Low-Power Logic. *Transducers Eurosens. XXVII, Int. Conf. Solid-State Sens., Actuators Microsyst., 17th* **2013**, 896−899.

(11) Qian, Y.; Soon, B. W.; Singh, P.; Campanella, H.; Lee, C. All Metal Nanoelectromechanical Switch Working at 300 °C for Rugged Electronics Applications. *Nanoscale* **2014**, *6*, 5606−5611.

(12) Chen, Y.; Nathanael, R.; Jeon, J.; Yaung, J.; Hutin, L.; Liu, T. J. K. Characterization of Contact Resistance Stability in MEM Relays with Tungsten Electrodes. *J. Microelectromech. Syst.* **2012**, *21*, 511−513.

(13) Ramezani, M.; Severi, S.; Moussa, A.; Osman, H.; Tilmans, H.; De Meyer, K. Contact Reliability Improvement of a Poly-SiGe based Nano-Relay with Titanium Nitride Coating. *Transducers 2015 - Int. Conf. Solid-State Sens., Actuators Microsyst., 17th* **2015**, 576−579.

(14) Coutu, R. A.; Reid, J. R.; Cortez, R.; Strawser, R. E.; Kladitis, P. E. Microswitches with Sputtered Au, AuPd, Au-on-AuPt, and AuPtCu Alloy Electric Contacts. *IEEE Trans. Compon. Packag. Technol.* **2006**, *29*, 341−349.

(15) He, T.; Yang, R.; Rajgopal, S.; Tupta, M. A.; Bhunia, S.; Mehregany, M.; Feng, P. X. Robust Silicon Carbide (SiC) Nanoelectromechanical Switches with Long Cycles in Ambient and High Temperature Conditions. *Proceedings of 2013 IEEE 26th International Conference on Micro Electro Mechanical Systems (MEMS)* **2013**, 516−519.

(16) He, T.; Yang, R.; Ranganathan, V.; Rajgopal, S.; Tupta, M. A.; Bhunia, S.; Mehregany, M.; Feng, P. X. Silicon Carbide (SiC) Nanoelectromechanical Switches and Logic Gates with Long Cycles and Robust Performance in Ambient Air and at High Temperature. *IEEE Int. Electron Devices Meet., 2013* **2013**, 4.6.1−4.6.4.

(17) Kam, H.; Pott, V.; Nathanael, R.; Jeon, J.; Alon, E.; Liu, T.-J. K. Design and Reliability of a Micro-Relay Technology for Zero-

Standby-Power Digital Logic Applications. *IEEE Int. Electron Devices Meet., 2009* **2009**, 1−4.
(18) Toler, B. F.; Coutu Jr, R. A.; McBride, J. W. A Review of Micro-Contact Physics for Microelectromechanical Systems (MEMS) Metal Contact Switches. *J. Micromech. Microeng.* **2013**, *23*, 103001.
(19) Seo, M.-H.; Ko, J.-H.; Lee, J. O.; Ko, S.-D.; Mun, J. H.; Cho, B. J.; Kim, Y.-H.; Yoon, J.-B. >1000-Fold Lifetime Extension of a Nickel Electromechanical Contact Device via Graphene. *ACS Appl. Mater. Interfaces* **2018**, *10*, 9085−9093.
(20) Rana, S.; Reynolds, J. D.; Ling, T. Y.; Shamsudin, M. S.; Pu, S. H.; Chong, H. M. H.; Pamunuwa, D. Nano-Crystalline Graphite for Reliability Improvement in MEM Relay Contacts. *Carbon* **2018**, *133*, 193−199.
(21) Choi, J.; Lee, J. I.; Eun, Y.; Kim, M. O.; Kim, J. Aligned Carbon Nanotube Arrays for Degradation-Resistant, Intimate Contact in Micromechanical Devices. *Adv. Mater.* **2011**, *23*, 2231−2236.
(22) Voevodin, A. A.; Vaia, R. A.; Patton, S. T.; Diamanti, S.; Pender, M.; Yoonessi, M.; Brubaker, J.; Hu, J.-J.; Sanders, J. H.; Phillips, B. S.; MacCuspie, R. I. Nanoparticle-Wetted Surfaces for Relays and Energy Transmission Contacts. *Small* **2007**, *3*, 1957−1963.
(23) Patton, S. T.; Slocik, J. M.; Campbell, A.; Hu, J.; Naik, R. R.; Voevodin, A. A. Bimetallic Nanoparticles for Surface Modification and Lubrication of MEMS Switch Contacts. *Nanotechnology* **2008**, *19*, 405705.
(24) Patton, S. T.; Voevodin, A. A.; Vaia, R. A.; Pender, M.; Diamanti, S. J.; Phillips, B. Nanoparticle Liquids for Surface Modification and Lubrication of MEMS Switch Contacts. *J. Microelectromech. Syst.* **2008**, *17*, 741−746.
(25) Ko, S.; Seo, M.; Yoon, Y.; Han, C.; Lim, K.; Kim, C.; Yoon, J. Investigation of the Nanoparticle Electrical Contact Lubrication in MEMS Switches. *J. Microelectromech. Syst.* **2017**, *26*, 1417−1427.
(26) Kageyama, T.; Shinozaki, K.; Zhang, L.; Lu, J.; Takaki, H.; Lee, S.-S. Fabrication of an Au−Au/Carbon Nanotube-Composite Contacts RF-MEMS Switch. *Micro Nano Syst. Lett.* **2018**, *6*, 6.
(27) Jo, E.; Seo, M.-H.; Pyo, S.; Ko, S.-D.; Kwon, D.-S.; Choi, J.; Yoon, J.-B.; Kim, J. Integration of a Carbon Nanotube Network on a Microelectromechanical Switch for Ultralong Contact Lifetime. *ACS Appl. Mater. Interfaces* **2019**, *11*, 18617−18625.
(28) Sun, K.; Stroscio, M. A.; Dutta, M. Graphite C-axis Thermal Conductivity. *Superlattices Microstruct.* **2009**, *45*, 60−64.
(29) Yang, D. J.; Wang, S. G.; Zhang, Q.; Sellin, P. J.; Chen, G. Thermal and Electrical Transport in Multi-Walled Carbon Nanotubes. *Phys. Lett. A* **2004**, *329*, 207−213.
(30) Jo, E.; Lee, Y.; Lee, J.; Kim, S.; Kim, W.; Seo, M.; Yoon, J.; Kim, J. Gold-Decorated Carbon Nanotube Network as Contact Surface of MEM Switch for Extended Lifetime. *IEEE Int. Conf. Micro Electro Mech. Syst., 32nd* **2019**, 958−961.
(31) Soltman, D.; Subramanian, V. Inkjet-Printed Line Morphologies and Temperature Control of the Coffee Ring Effect. *Langmuir* **2008**, *24*, 2224−2231.
(32) Weizmann, Y.; Lim, J.; Chenoweth, D. M.; Swager, T. M. Regiospecific Synthesis of Au-Nanorod/SWCNT/Au-Nanorod Heterojunctions. *Nano Lett.* **2010**, *10*, 2466−2469.
(33) Ozhikandathil, J.; Badilescu, S.; Packirisamy, M. Plasmonic Gold Decorated MWCNT Nanocomposite for Localized Plasmon Resonance Sensing. *Sci. Rep.* **2015**, *5*, 13181.
(34) Baek, D.-H.; Kim, J. MoS2 Gas Sensor Functionalized by Pd for the Detection of Hydrogen. *Sens. Actuators, B* **2017**, *250*, 686−691.
(35) Ko, S.-D.; Oen Lee, J.; Yang, H.-H.; Kim, M.-W.; Song, Y.-H.; Yoon, J.-B. An Insulating Liquid Environment for Reducing Adhesion in a Microelectromechanical System. *Appl. Phys. Lett.* **2011**, *99*, 113516.
(36) Lee, J. O.; Song, Y.-H.; Kim, M.-W.; Kang, M.-H.; Oh, J.-S.; Yang, H.-H.; Yoon, J.-B. A Sub-1-V Nanoelectromechanical Switching Device. *Nat. Nanotechnol.* **2013**, *8*, 36−40.
(37) Dong, K.; Choe, H. S.; Wang, X.; Liu, H.; Saha, B.; Ko, C.; Deng, Y.; Tom, K. B.; Lou, S.; Wang, L.; Grigoropoulos, C. P.; You, Z.; Yao, J.; Wu, J. A 0.2 V Micro-Electromechanical Switch Enabled by a Phase Transition. *Small* **2018**, *14*, 1703621.
(38) Lee, J. O.; Choi, K.-W.; Choi, S.-J.; Kang, M.-H.; Seo, M.-H.; Kim, I.-D.; Yu, K.; Yoon, J.-B. Nanomechanical Encoding Method Using Enhanced Thermal Concentration on a Metallic Nanobridge. *ACS Nano* **2017**, *11*, 7781−7789.
(39) Zaghloul, U.; Piazza, G. Sub-1-V Piezoelectric Nanoelectromechanical Relays With Millivolt Switching Capability. *IEEE Electron Device Lett.* **2014**, *35*, 669−671.
(40) Qian, C.; Peschot, A.; Osoba, B.; Ye, Z. A.; Liu, T. K. Sub-100 mV Computing With Electro-Mechanical Relays. *IEEE Trans. Electron Devices* **2017**, *64*, 1323−1329.
(41) Osoba, B.; Saha, B.; Dougherty, L.; Edgington, J.; Qian, C.; Niroui, F.; Lang, J. H.; Bulovic, V.; Wu, J.; Liu, T. K. Sub-50 mV NEM Relay Operation Enabled by Self-Assembled Molecular Coating. *IEEE Int. Electron Devices Meet., 2016* **2016**, 26.8.1−26.8.4.
(42) Cao, Q.; Tersoff, J.; Farmer, D. B.; Zhu, Y.; Han, S.-J. Carbon Nanotube Transistors Scaled to a 40-nanometer Footprint. *Science* **2017**, *356*, 1369.
(43) Jang, W. W.; Lee, J. O.; Yoon, J.-B.; Kim, M.-S.; Lee, J.-M.; Kim, S.-M.; Cho, K.-H.; Kim, D.-W.; Park, D.; Lee, W.-S. Fabrication and Characterization of a Nanoelectromechanical Switch with 15-nm-Thick Suspension Air Gap. *Appl. Phys. Lett.* **2008**, *92*, 103110.
(44) Saha, S.; Singh, A.; Baghini, M. S.; Goel, M.; Rao, V. R. Standby Power Reduction Using Experimentally Demonstrated Nano-Electromechanical Switch in CMOS Technologies. *IEEE Trans. Electron Devices* **2021**, *68*, 746−752.
(45) Lee, D.; Lee, B.-H.; Yoon, J.; Ahn, D.-C.; Park, J.-Y.; Hur, J.; Kim, M.-S.; Jeon, S.-B.; Kang, M.-H.; Kim, K.; Lim, M.; Choi, S.-J.; Choi, Y.-K. Three-Dimensional Fin-Structured Semiconducting Carbon Nanotube Network Transistor. *ACS Nano* **2016**, *10*, 10894−10900.
(46) Wang, Y.; Liu, F.; Zhang, X. Flexible Transfer of Plasmonic Photonic Structures onto Fiber Tips for Sensor Applications in Liquids. *Nanoscale* **2018**, *10*, 16193−16200.
(47) Tas, N.; Sonnenberg, T.; Jansen, H.; Legtenberg, R.; Elwenspoek, M. Stiction in Surface Micromachining. *J. Micromech. Microeng.* **1996**, *6*, 385−397.
(48) Seo, M.-H.; Jo, E.; Ko, S.-D.; Choi, J.; Yoon, Y.-H.; Kwon, D.-S.; Kim, J.; Yoon, J.-B. Carbon Nanotubes Network Contact Lubrication for Highly Reliable MEMS Switch. *IEEE Int. Conf. Micro Electro Mech. Syst., 30th* **2017**, 5−8.

https://doi.org/10.1021/acsami.0c22084
ACS Appl. Mater. Interfaces 2021, 13, 16959−16967